

# The Linkage of Catalysis and Regulation in Enzyme Action. Solvent Isotope Effects as Probes of Protonic Sites in the Yeast Pyruvate Decarboxylase Mechanism<sup>1</sup>

Francisco J. Alvarez,<sup>†</sup> Joachim Ermer,<sup>‡</sup> Gerhard Hübner,<sup>‡</sup>  
Alfred Schellenberger,<sup>‡</sup> and Richard L. Schowen<sup>\*†</sup>

Contribution from the Departments of Chemistry and Biochemistry and the Higuchi Biosciences Center, University of Kansas, Lawrence, Kansas 66045-0046, and Institute for Biochemistry, Martin Luther University of Halle-Wittenberg, Weinbergweg 16a, D-06099 Halle/Saale, Federal Republic of Germany

Received November 11, 1994<sup>®</sup>

**Abstract:** Yeast pyruvate decarboxylase, a thiamin-diphosphate-dependent enzyme which undergoes slow hysteretic activation by its own substrate pyruvate to form an active enzyme that cycles several thousand times before deactivation, exhibits rate constants (a) 2-fold larger in deuterium oxide than in protium oxide for the second-order kinetic term in pyruvate ( $k/A$ ), (b) 2.3-fold larger in deuterium oxide for the first-order term in pyruvate ( $k/B$ ), and (c) 1.5-fold larger in protium oxide than in deuterium oxide for the zero-order term in pyruvate. Proton inventories (rates in mixtures of protium and deuterium oxides) for  $k/A$  and  $k/B$  suggest that the isotope effects arise from addition of an enzymic sulfhydryl group to the regulatory pyruvate preceding the transition state for combination of pyruvate with the activated enzyme, with the addition reaction occurring in every catalytic cycle. The proton inventory for  $k$  is consistent with sulfhydryl addition to the regulatory pyruvate, coupled to a multiproton process in the transition state for release of the product acetaldehyde. A model for regulation is suggested in which the opening and closing of sequestering structures at the active site are driven by sulfhydryl addition/elimination reactions at the carbonyl group of the regulatory pyruvate molecule.

## Introduction

Pyruvate decarboxylase of the yeast *Saccharomyces cerevisiae* (SCPDC; pyruvate carboxylase, EC 4.1.1.1) is a thiamin-diphosphate (TDP)-dependent enzyme that catalyzes the reaction shown in Figure 1. SCPDC exists as a tetramer with four MgTDP molecules tightly bound. There is an extensive mechanistic background about the yeast enzyme,<sup>2–7</sup> and crystal structures have recently become available.<sup>3</sup> The enzyme is hysteretically regulated by the substrate,<sup>1,2</sup> being slowly activated

<sup>†</sup> University of Kansas.

<sup>‡</sup> Martin Luther University.

<sup>®</sup> Abstract published in *Advance ACS Abstracts*, February 1, 1995.

(1) For preliminary reports on some aspects of the work presented in this paper, see: (a) Ermer, J.; Hübner, G.; Schellenberger, A. *Biochem. Physiol. Thiamin Diphosphate Enzymes, Proc. Int. Meet. Funct. Thiamin Diphosphate Enzymes* 1991, 67–76. (b) Alvarez, F. J.; Schowen, R. L. In *Thiamin Pyrophosphate Biochemistry*; Schellenberger, A., Schowen, R. L., Eds.; CRC Press: Boca Raton, FL, 1988; Vol. I, pp 101–112. The work in the USA was supported by NIH Grant No. GM-20198.

(2) Kluger, R. *Chem. Rev.* 1987, 87, 863–876. Bisswanger, H., Ullrich, J., Eds. *The Biochemistry and Physiology of Thiamin Diphosphate Enzymes*; VCH Publishers: Weinheim, 1991.

(3) (a) Dyda, F.; Furey, W.; Swaminathan, S.; Sax, M.; Farrenkopf, B.; Jordan, F. *Biochemistry* 1993, 32, 6165–6170. (b) Muller, Y. A.; Lindqvist, Y.; Furey, W.; Schulz, G. E.; Jordan, F.; Schneider, G. *Structure (London)* 1993, 1, 95–103. (c) Lindqvist, Y.; Schneider, G. *Curr. Opin. Struct. Biol.* 1993, 3, 896–901. (d) König, S.; Schellenberger, A.; Neef, H.; Schneider, G. *J. Biol. Chem.* 1994, 269, 10879–10882 and references given in these papers.

(4) Alvarez, F. J.; Ermer, J.; Hübner, G.; Schellenberger, A.; Schowen, R. L. *J. Am. Chem. Soc.* 1991, 113, 8402–8409.

(5) Huhta, D. W.; Heckenthaler, T.; Alvarez, F. J.; Ermer, J.; Hübner, G.; Schellenberger, A.; Schowen, R. L. *Acta Chem. Scand.* 1992, 46, 778–788.

(6) Baburina, I.; Gao, Y.; Hu, Z.; Jordan, F.; Hohmann, S.; Furey, W. *Biochemistry* 1994, 33, 5630–5635 and references therein. See, also: Schellenberger, A.; Hübner, G.; Sieber, M. In *Thiamin Pyrophosphate Biochemistry*; Schellenberger, A., Schowen, R. L., Eds.; CRC Press: Boca Raton, FL, 1988; Vol. I, pp 113–121. Hübner, G.; König, S.; Schellenberger, A. *Biomed. Biochim. Acta* 1988 47, 9–18.

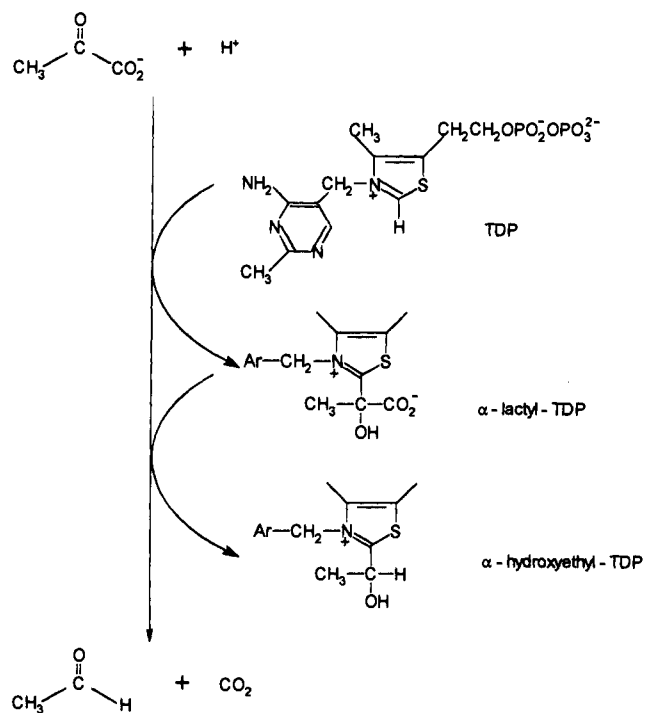


**Figure 1.** Decarboxylation of pyruvate anion as catalyzed by SCPDC with employment of the cofactor TDP. For a discussion of the detailed mechanistic features and in particular of issues connected with the reactant adduct  $\alpha$ -lactyl-TDP and the product adduct  $\alpha$ -(hydroxyethyl)-TDP, see the review by Kluger.<sup>2</sup>

by a regulatory pyruvate molecule and then cycling several thousands of times through the catalytic sequence before a deactivation event occurs.<sup>2,4,5</sup> A kinetic scheme depicting the steps in activation and catalysis is shown in Figure 2; the scheme

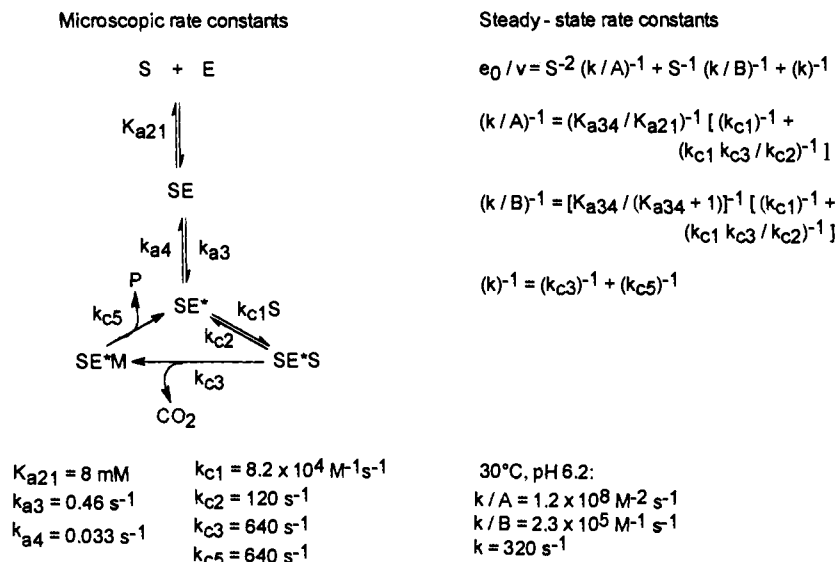


**Figure 2.** At top left, a minimal mechanistic scheme for regulatory activation (vertical stem) and catalysis (triangular base) manifolds of the SCPDC reaction. S is pyruvate, E the inactive SCPDC, SE\* the substrate-activated SCPDC complex, SE\*S the accumulating species that precedes decarboxylation, and SE\*M the accumulating species that precedes product release. The accumulating species cannot at present be specified structurally, e.g., SE\*M may contain  $\alpha$ -(hydroxyethyl)-TDP, the conjugate base of this species, acetaldehyde and TDP or other structures. The microscopic rate constants obtained<sup>4,5</sup> by transient kinetic studies (activation) and deduction from hydrogen and carbon isotope effects (catalysis) are shown below the scheme. (The term "microscopic rate constant" refers to a rate constant for a step or combination of steps in the reaction mechanism, which is not directly accessible from the steady-state kinetics; aggregates of microscopic rate constants form the steady-state rate constants, which are experimentally obtainable from kinetic studies.) At right, the steady-state kinetic law is shown in reciprocal form at the top. Substrate inhibition, which can enter at very high [pyruvate], is omitted but is included in eq 1 in the text. Each of the three steady-state rate constants,  $k/A$  (second order in pyruvate),  $k/B$  (first order in pyruvate), and  $k$  (zero order in pyruvate), is then shown in reciprocal form in its relationship to the microscopic rate and equilibrium constants. Note that the quantities  $A$  and  $B$  are constants analogous to  $K_m$  values, with units of  $M^2$  and  $M$ , respectively. At bottom right are previously obtained<sup>4</sup> values of the steady-state constants.

shows notation for the microscopic rate constants in the activation (subscript a) and catalysis (subscript c) manifolds and the relationship of these to the steady-state rate constants.<sup>4,5</sup>

In the previous work, we made use of substrate-<sup>13</sup>C primary isotope effects and substrate-CD<sub>3</sub>  $\beta$ -deuterium secondary isotope effects to estimate the rate constants for individual steps in the enzymic reaction sequence<sup>4</sup> and we compared these with the rate constants for the nonenzymic reaction to obtain information about how the enzyme stabilizes transition states and reactant states.<sup>5</sup> The estimated microscopic rate constants and measured steady-state rate constants are shown in Figure 2.

Solvent isotope effects on PDC action should aid in characterizing those steps likely to involve exchangeable protic sites. The regulatory mechanism is thought to involve sulfhydryl addition to the regulatory pyruvate carbonyl groups,<sup>6</sup> and it has been suggested<sup>7</sup> that sulfhydryl groups are variously involved in the catalytic mechanism. We report here solvent isotope effects for activation of and catalysis by SCPDC. The results suggest a way in which regulatory events may be coupled to catalytic events.

## Results

**Steady-State Kinetic Parameters in Protium and Deuterium Oxides.** The kinetic law for SCPDC includes three kinetic parameters, defined in Figure 2. Substrate inhibition<sup>4</sup> is observed under some circumstances and requires the inclusion of an inhibition constant,  $K_i$ . Steady-state initial velocities  $v$  were determined as before<sup>4</sup> (coupling of acetaldehyde production to alcohol dehydrogenase action) and fitted to eq 1 by nonlinear least-squares procedures. In cases where substrate inhibition

was not detected,  $S/K_i$  in eq 1 was set equal to zero.

$$v/e_0 = S^2/\{(A/k) + S(B/k) + S^2(1/k)[1 + S/K_i]\} \quad (1)$$

To normalize the varying enzyme activities in the different experiments, the values of  $k$  were adjusted to a common value of  $320 \text{ s}^{-1}$  at pH 6.2, corresponding to an activity of pure SCPDC of 80 units/mg and taking the active entity as the tetramer (so that the value will become  $80 \text{ s}^{-1}$  per TDP site).<sup>4</sup> In some cases, approximate values of  $k$  were obtained by measuring velocities at 20 mM pyruvate (where  $S^2/A = 150$ ,  $S/B = 14$ , and  $S/K_i = 0.08$ ).

Limited data were obtained on the steady-state parameters as functions of pH in protium oxide (HOH) and pD in deuterium oxide (DOD) and are given in the supplementary material. The rate constants  $k/A$  and  $k/B$  both decline with increasing pL in HOH and DOD with apparent pK values for  $k/A$  of 6.0 (HOH) and 6.5 (DOD) and for  $k/B$  of 6.0 (HOH) and 6.6 (DOD). Thus the expected<sup>8,9</sup> pK shift of 0.5–0.6 unit to the basic in DOD is observed in both cases. The apparent limiting rate constants at low pL are for  $k/A$   $1.4 \times 10^8 \text{ M}^{-2} \text{ s}^{-1}$  (DOD) and  $0.7 \times 10^8 \text{ M}^{-2} \text{ s}^{-1}$  (HOH) and for  $k/B$   $1.5 \times 10^6 \text{ M}^{-1} \text{ s}^{-1}$  (DOD) and  $0.65 \times 10^6 \text{ M}^{-1} \text{ s}^{-1}$  (HOH). Thus the inverse solvent isotope effects are similar for  $k/A$  (2-fold faster in DOD) and for  $k/B$  (2.3-fold faster in DOD). The rate constant  $k$  exhibits a maximum in rate around pH 6 and pD 6.5 (pKs approximately 5.2 and 7.5 in HOH and 5.8 and 8.1 in DOD, both thus

(8) Schowen, K. B.; Schowen, R. L. *Methods Enzymol.* **1982**, 87C, 551–606.

(9) Quinn, D. M.; Sutton, L. D. In *Enzyme Mechanism from Isotope Effects*; Cook, P. F., Ed.; CRC Press: Boca Raton, FL, 1991.

(10) Cleland, W. W.; Kreevoy, M. M. *Science* **1994**, 264, 1887–1890.

(11) Northrop et al. have previously noted and discussed (Cho, Y.-K.; Rebbholz, K. L.; Northrop, D. B. *Biochemistry* **1994**, 33, 9637–9642) the effects of loosely bound reactant-state sites on proton inventories.

(7) Jordan, F.; Akinyosoye, O.; Dikdan, G.; Kudzin, Z.; Kuo, D. In *Thiamine Pyrophosphate Biochemistry*; Schellenberger, A., Schowen, R. L., Eds.; CRC Publishers: Boca Raton, FL, 1988; Vol. 1, pp 79–92. Schellenberger, A.; Hübner, G.; Sieber, M. *Ibid.* 113–121.

**Table 1.** Proton Inventory Data for Steady-State Kinetic Parameters in the Action of Pyruvate Decarboxylase

rate constants, units, reaction conditions	rate constant value [SD], atom fraction of deuterium <i>n</i> in HOH/DOD mixtures
$10^{-6}k/A$ , $M^{-2} s^{-1}$ , 30.00 ± 0.05 °C, 0.1000 M citrate buffer, pH 6.3, and equivalent pL	117[4], 0.00; 126[6], 0.15; 139[8], 0.30; 157[5], 0.40; 161[6], 0.50; 163[4], 0.60; 180[4], 0.70; 208[4], 0.85; 236[5], 0.98
$10^{-4}k/B$ , $M^{-1} s^{-1}$ , 30.00 ± 0.05 °C, 0.1000 M citrate buffer, pH 6.3, and equivalent pL	23[2], 0.00; 26[2], 0.15; 28[3], 0.30; 28[3], 0.40; 34[5], 0.50; 36[3], 0.60; 40[3], 0.70; 49[3], 0.85; 54[4], 0.98
$k$ , $s^{-1}$ , 30.00 ± 0.05 °C, 0.1000 M citrate buffer, pH 6.3, and equivalent pL	320[3], 0.00; 287[3], 0.15; 259[3], 0.30; 254[3], 0.40; 238[2], 0.50; 235[2], 0.60; 226[1], 0.70; 218[1], 0.85; 210[1], 0.98
$k$ , $s^{-1}$ , 25.0 ± 0.2 °C, 0.100 M citrate buffer, pH 6.3, and equivalent pL	320[6], 0.00; 301[6], 0.10; 288[6], 0.20; 275[5], 0.30; 262[5], 0.40; 253[5], 0.50; 237[5], 0.60; 230[5], 0.70; 224[4], 0.80; 221[4], 0.94

exhibiting a reasonable  $\Delta pK$  around 0.6). The limiting value of  $k$  is approximately  $370 s^{-1}$  (HOH) and  $270 s^{-1}$  (DOD), yielding a normal isotope effect of 1.4. The pH(D) dependencies for  $k/A$ ,  $k/B$ , and  $k$  are consistent with normal behavior<sup>8,9</sup> for SCPDC and thus its structural integrity in DOD. This, in turn, supports a straightforward interpretation of the solvent isotope effects and proton inventories.

**Steady-State Kinetic Parameters in Mixtures of Protium and Deuterium Oxides.** In order to make use of the proton inventory approach<sup>8,9</sup> to interpret the solvent isotope effects, the steady-state kinetics were determined in mixtures of protium and deuterium oxides. For each atom fraction  $n$  of deuterium, initial rates were measured and fitted to eq 1 as described above. Alternatively, saturating concentrations of pyruvate were used to obtain approximate values of  $k$ . The data are shown in Table 1.

**Kinetics and Solvent Isotope Effects for Activation of SCPDC.** The rate and equilibrium constants for the regulatory activation and deactivation manifold were determined from the transient kinetics over a small range of pL with low precision (10–20% for  $K_{a21}$ ; ca. 10% for  $k_{a3}$  and  $k_{a4}$ ). The results are given in the supplementary material. Briefly, the findings indicate little or no solvent isotope effect associated with the slow regulatory activation/deactivation processes. The apparent equilibrium constant  $K_{a21}$  for dissociation of the regulatory pyruvate from the regulatory site changes little with pL = pH(D) and exhibits no solvent isotope effect (mean values over the pL range,  $7.3 \pm 1.5$  mM in HOH and  $7.8 \pm 2.5$  mM in DOD). The values of both  $k_{a3}$  and  $k_{a4}$ , the “on-switching” and “off-switching” rate constants, respectively, for the activating transition, appear to decrease in a similar manner with increasing pL, possibly with a pK in the range 6–6.5 in HOH and 6.5–7 in DOD. Estimates of  $k_{a3\text{HOH}}/k_{a3\text{DOD}} = 1.0\text{--}1.6$  and  $k_{a4\text{HOH}}/k_{a4\text{DOD}} = 1.3\text{--}2.1$ , so that if there are solvent isotope effects on either, they are not greatly different. This leads to solvent isotope effects of 0.6–1.2 for the equilibrium constant  $K_{a34}$  of the activating transition, averaging to about  $0.8 \pm 0.2$ . Values of  $K_{a34}$  itself are  $14 \pm 3$  in HOH.

## Discussion

**Proton Inventories for  $k/A$  and  $k/B$ .** Figure 3 shows proton inventories<sup>8,9</sup> (plots of rate constant vs  $n$ , the atom fraction of

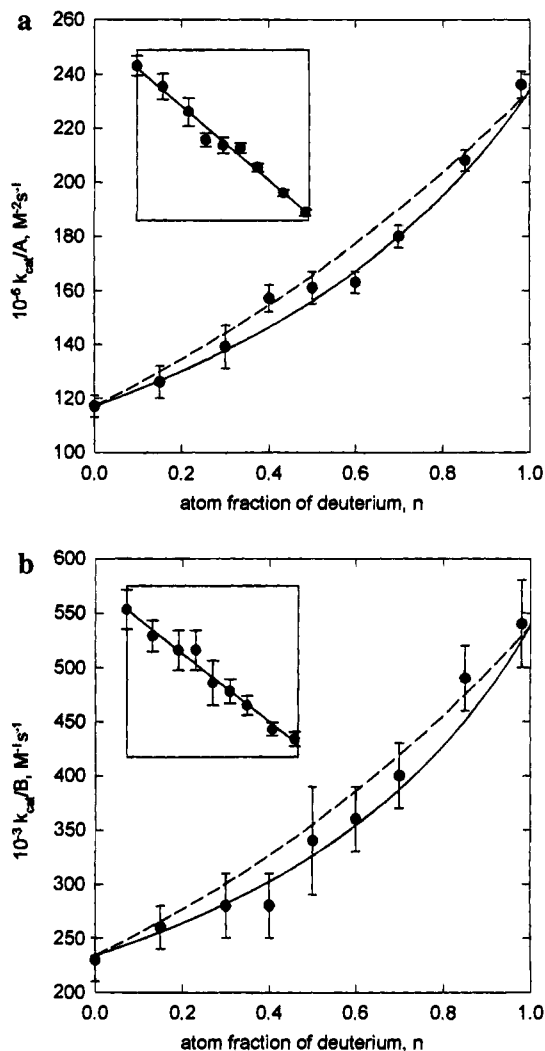


**Figure 3.** Proton inventories for (a)  $k/A$  and (b)  $k/B$ . The solid curves are plots of eqs 2a,b, respectively. The dashed lines are exponential relationships that ascribe the isotope effect to generalized solvation or protein conformational changes. The insets show plots of the reciprocal rate constants vs  $n$ ; as eqs 2a,b show, such plots should be linear.

deuterium in mixtures of protium and deuterium oxides) for the steady-state rate constants  $k/A$  and  $k/B$ . The rate constants were measured at “equivalent pL”, i.e., with the same buffer acid/base ratio in all isotopic solvents, so that the data refer to the same fraction of active enzyme in all isotopic solvents.<sup>8,9</sup> The rate constants are larger in deuterium oxide by factors of 2 ( $k/A$ ) and 2.3 ( $k/B$ ).

Both rate constants depend nonlinearly on  $n$ . This suggests that conversion of a water-like site ( $\phi = 1$ ) in the reactant state to a “tight” protonic site in the transition state does not generate the inverse isotope effects: such a model would produce a linear proton inventory.<sup>8,9</sup> Furthermore, the data are not consistent with a generalized solvation or protein conformational change. This would generate an exponential proton inventory (dashed lines in Figure 3).

The rate constants  $k/A$  and  $k/B$  are related in part to the regulatory manifold (see below). Baburina et al.<sup>6</sup> have shown a cysteine residue (221) to be required for regulation, and it is known<sup>1,2,4–6</sup> that binding of a regulatory pyruvate molecule to SCPDC is required for activation. Since fractionation factors of  $(1/2)\text{--}(1/2.3)$  are around that expected<sup>8,9</sup> for a sulfhydryl group, the hypothesis can be considered that a free reactant-state sulfhydryl group undergoes complete carbonyl addition to a regulatory pyruvate before the effective transition state for

$k/A$  or  $k/B$ , generating the inverse isotope effects. This predicts the  $n$ -dependences of eqs 2a,b for  $k/A$  and  $k/B$ , respectively.

$$10^{-6}k/A \text{ (M}^{-2} \text{ s}^{-1}\text{)} = 117/(1 - n + n/[2]) \quad (2a)$$

$$10^{-3}k/B \text{ (M}^{-1} \text{ s}^{-1}\text{)} = 234/(1 - n + n/[2.3]) \quad (2b)$$

Note that the quantitative predictions of these two equations make use only of the rate constants in protium oxide (rate constant at  $n = 0$ ) and the overall isotope effects. Nevertheless, as Figure 3 shows, the predicted  $n$ -dependences give an excellent account of the measurements at all values of  $n$  for both  $k/A$  and  $k/B$ . The reciprocals of eqs 2a,b should be linear in  $n$ . The insets to Figure 3 show that this expectation is also met. Furthermore, alternative models including a generalized change in protein structure (dashed lines in Figure 3) do not fit the data nearly so well.

The interpretation of the proton inventories on  $k/A$  and  $k/B$  as indicative of addition of an active site sulfhydryl to the carbonyl group of the regulatory pyruvate molecule is therefore based on the following lines of evidence: (a) the proton-inventory data are strongly consistent with the sulfhydryl model in both cases and far less so with the generalized solvation model (Figure 3); (b) the C221S mutant is devoid of regulatory properties, showing C221 to be involved in regulation;<sup>6</sup> (c) previous studies with alternative regulators such as pyruvamide and with enzymes modified at sulfhydryl also support a regulatory addition of sulfhydryl to pyruvate;<sup>2,6</sup> and (d) the  $\beta$ -deuterium isotope effects,<sup>4</sup> as discussed below, show that carbonyl addition at a single pyruvate carbonyl group is occurring before the transition state for  $k/A$  and for  $k/B$ . These lines of evidence, taken together, support the sulfhydryl addition hypothesis and argue against alternative interpretations of the proton inventories.

This result is strongly consistent with models in which a "loosely bound" reactant-state site such as a sulfhydryl group has become a "tightly bound" transition-state site such as a hydroxyl group, as would occur if a sulfhydryl group at the regulatory site underwent addition to the carbonyl group of the regulatory pyruvate molecule to form the S-( $\alpha$ -lactyl) adduct.<sup>6</sup> In principle, these inverse isotope effects are also consistent with loss of a reactant-state "low-barrier hydrogen bond",<sup>10</sup> but the observation<sup>6</sup> that regulation depends on the presence of cysteine 221 of SCPDC makes the sulfhydryl site a better candidate.

Such a regulatory sulfhydryl addition reaction may be linked to the entry of the catalytic pyruvate into the active site. This conclusion depends on (a) the proton inventory results, (b) the magnitude of the activation manifold "on-switching" equilibrium constant  $K_{a34}$ , and (c) the substrate isotope effects determined in earlier work.<sup>4</sup>

The rate constant  $k/A$  (see Figure 2 for its definition) describes the overall conversion of the reactant state  $2S + E$  to, in principle, the transition states for  $k_{c1}$  and  $k_{c3}$ . However, the <sup>13</sup>C isotope effect for this term is only about 0.8–0.9% (discussed previously<sup>4</sup>) so that the decarboxylation transition state is less than 20% rate-limiting.<sup>4</sup> Thus the effective transition state for  $k/A$  is essentially that for  $k_{c1}$ . Although we describe the  $k_{c1}$  process by a single rate constant, events including entry of pyruvate into the active site, addition of pyruvate to TDP, and possible protein conformation changes may contribute. The proton inventory result is consistent with the completion of an equilibrium addition of sulfhydryl to carbonyl, presumably at

the regulatory site, at any point between the reactant state  $2S + E$  and the transition state for  $k_{c1}$ . In earlier work,<sup>4</sup> the  $\beta$ -deuterium secondary isotope effect for  $CD_3COCOOH$  was measured as  $0.883 \pm 0.013$ . The value corresponds<sup>4</sup> to about the value expected for a single, completed equilibrium addition to carbonyl, such as the regulatory sulfhydryl addition. A more inverse isotope would have been expected if nucleophilic interaction were occurring at the second, active-site pyruvate. The observed isotope effect thus means, most simply, that between  $2S + E$  and the transition state for  $k_{c1}$  equilibrium addition of sulfhydryl to the regulatory pyruvate carbonyl group has been completed *but few or no other bonding changes that would generate a  $\beta$ -secondary isotope effect have occurred*. The addition of TDP to the active site pyruvate, in particular, must be contributing very little to the transition state for  $k_{c1}$ . The transition state for  $k/A$  therefore corresponds most simply to that for the entry of pyruvate into the active site.

The rate constant  $k/B$  (see Figure 2 for its definition) refers to the same transition state as  $k/A$  and thus essentially to the transition state for  $k_{c1}$ . This transition state, as just argued, is that for pyruvate entry into the active site. The proton inventory for  $k/B$  is again consistent with an equilibrium sulfhydryl addition reaction at the carbonyl of the regulatory pyruvate that precedes the transition state. This conclusion is again confirmed by the  $\beta$ -deuterium secondary isotope effect<sup>4</sup> for  $k/B$  of  $0.881 \pm 0.026$ . The reactant state for  $k/B$  could, in principle, be either  $S + SE$  or  $S + SE^*$  or both, depending on the magnitude of the constant  $K_{a34}$  (see Figure 2). The value of  $K_{a34}$  is  $14 \pm 3$ , showing that the pool of  $SE + SE^*$  consists of 14/15 or more than 90%  $SE^*$ , which is therefore the effective reactant state for  $k/B$ . Thus *the regulatory sulfhydryl addition reaction is occurring not between  $SE$  and  $SE^*$  but within the catalytic cycle, between  $SE^*$  and the transition state for  $k_{c1}$* .

Previously, the sulfhydryl addition reaction has been thought<sup>4</sup> to be the chemical event that triggered the slow conversion of  $SE$  to  $SE^*$ . In fact, the slow activating transition of the enzyme (the  $k_{a3}$  step in Figure 2) appears *not* to be coupled to sulfhydryl addition at the regulatory site. Instead, the addition reaction occurs after  $SE^*$  formation and thus within the catalytic cycle. It seems to occur before (and thus to be at equilibrium in) the transition state for the  $k_{c1}$  step. This transition state, as argued above, appears to involve little bonding change at the substrate (active site) carbonyl and is thus most easily envisioned as the transition state for entry of the pyruvate molecule into the active site. The combined results then suggest that the regulatory sulfhydryl addition reaction occurs before and is in some sense coupled to the process of admission of pyruvate into the active site.

Because the regulatory sulfhydryl addition occurs within the catalytic cycle, it follows that there must be an elimination reaction later within the catalytic cycle in order to restore the regulatory site to the free-sulfhydryl/free-carbonyl form before the entry of each new pyruvate molecule. We return to this point below.

**Proton Inventory for  $k$ .** Figure 4 shows a plot of  $k$  vs  $n$  for data obtained in both Halle and Lawrence but for slightly different temperatures (25 °C in Halle, 30 °C in Lawrence) and calculated on slightly different kinetic models (a very large substrate inhibition constant in Lawrence, an infinite substrate inhibition constant in Halle). The overall isotope effect is  $k(\text{HOH})/k(\text{DOD}) = 1.54$ .

The upper, straight line in the plot connects the rate constants in protium and deuterium oxides linearly. The lower, curved line connects the same points by an exponential function. These lines represent the two limiting cases<sup>8,9</sup> for simple interpretation

(12) Schneider, G.; Lindqvist, Y. *Bioorg. Chem.* **1993**, *21*, 109–117 and references therein.

(13) Crosby, J.; Stone, R.; Lienhard, G. E. *J. Am. Chem. Soc.* **1970**, *92*, 2891–2900. Crosby, J.; Lienhard, G. E. *Ibid.* **1970**, *92*, 5705–5716.

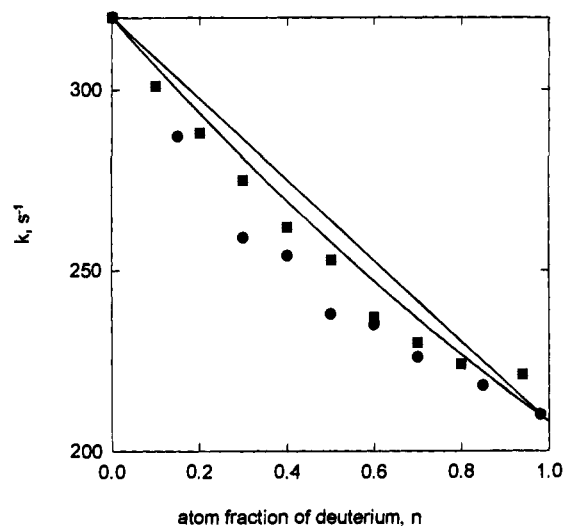


**Figure 4.** Proton inventory ( $k_n/n$ ) for the rate constant  $k$ . The rectangles represent data obtained in Halle by nonlinear least-squares fitting to eq 1 (with  $S/K_i = 0$ ) of initial rates measured at pL 6.3 and equivalent and 25 °C. The circles represent data obtained in Lawrence by nonlinear least-squares fitting to eq 1 (with  $K_i = 264$  mM) of initial rates measured at pL 6.2 and equivalent and 30 °C. Both data sets were adjusted to  $k_0 = 320$  s<sup>-1</sup> (activity of pure SCPDC = 80 U/mg). The upper curve is a straight line with  $k_1 = 208$  s<sup>-1</sup>. The lower curve is an exponential function with  $k_0 = 320$  s<sup>-1</sup> and  $k_1 = 208$  s<sup>-1</sup>. Probable error limits for repetitions of the measurements lie within the space of the symbols.

of proton inventories: a linear dependence signals a “one-proton” isotope effect, while an exponential dependence indicates an “infinite-proton” model in which many sites contribute small isotope effects, as in a generalized solvation change or protein conformational change.<sup>8,9</sup> These simple models apply<sup>8,9</sup> if these two conditions are met: (a) all reactant-state sites that contribute to the isotope effect are “water-like” ( $\phi = 1$ ) and (b) one step is fully rate-limiting, so that a single effective reactant state is transformed to a single effective transition state.

Of the 16 points in mixtures of isotopic waters, all but one fall below the exponential limit. This is an example of *hypercurvature* in the proton inventory, suggesting that conditions a and/or b in the preceding paragraph are not met.<sup>11</sup>

Indeed, we know that condition b is not met, for previous work<sup>4</sup> indicated that a single step does not limit the rate for  $k$ . Substrate isotope effects suggested (see the microscopic rate constants in Figure 2) that  $k$  (320 s<sup>-1</sup>) is determined about equally by decarboxylation ( $k_{c3} = 640$  s<sup>-1</sup>) and product release ( $k_{c5} = 640$  s<sup>-1</sup>). Therefore, we now consider a model according to which one of these two steps (probably decarboxylation) produces no isotope effect and maintains a rate constant of 640 s<sup>-1</sup> at all values of  $n$ . If this were true, the solvent isotope effect would come wholly from the product release process. This process, although we describe it by a single rate constant, consists in principle of a series of elementary steps, including protonation to generate  $\alpha$ -(hydroxyethyl)-TDP of the “enamine” species following decarboxylation, decomposition of  $\alpha$ -(hydroxyethyl)-TDP to generate acetaldehyde, release of the latter from the active site, protonation of the TDP C<sub>2</sub>-carbanion, and possible protein conformational changes.

On the model just described, the rate constant for product release in mixtures of HOH and DOD, which we will call  $q_n$ , is given by eq 3. The resulting values of  $q_n$  are plotted vs  $n$  in Figure 5a and continue to exhibit hypercurvature in the proton inventory.

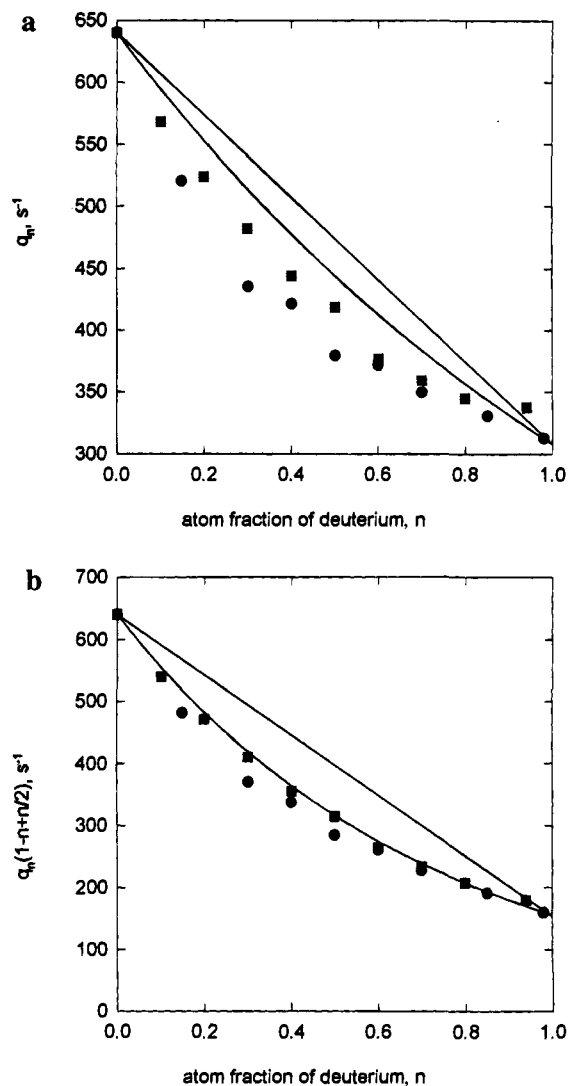


**Figure 5.** (a) Proton inventory for the presumed isotope-sensitive product release step, assuming that  $k_0$  describes two serial steps each with rate constant 640 s<sup>-1</sup>, that one of the steps (decarboxylation) has no isotope effect, and that the other step (product release) is isotope-sensitive. Thus the ordinate  $q_n$  (s<sup>-1</sup>) = 640 $k_n$ /(640 -  $k_n$ ). The upper curve is a straight line corresponding to a one-proton isotope effect of 2.1. The lower curve is an exponential function corresponding to a multiproton isotope effect of 2.1. (b) Demonstration that the proton inventory for the isotope-sensitive step can be described by the equation  $q_n$  (s<sup>-1</sup>) = 640(4.1)<sup>- $n$ /(1 -  $n$  +  $n$ /2)</sup>, which corresponds to an isotope effect of about 2 arising from partial cancellation of a multiproton contribution of 4 in the transition state by a reactant-state fractionation factor of 1/2. The ordinate is the product  $q_n(1 - n + n/2)$  so that the hypothesis dictates that the data should be an exponential function of  $n$ . The upper curve is the straight line corresponding to a one-proton isotope effect of 4.1. The lower curve is an exponential function corresponding to a multiproton isotope effect of 4.1.

$$q_n(\text{s}^{-1}) = 640k_n/(640 - k_n) \quad (3)$$

There is accordingly some further source of hypercurvature. A reasonable candidate is a failure of at least one of the reactant-state sites involved in catalysis to be “water-like” (condition a above).

Possibly a loosely bound reactant-state site such as a sulfhydryl group with isotopic fractionation factor<sup>8,9</sup> around 1/2 might be important in product release<sup>7</sup> as well as in substrate binding, as was shown above for  $k/A$  and  $k/B$ . This hypothesis implies the proton inventory expression of eq 4, where TSC means *transition-state contribution*.

$$q_n = \text{TSC}/(1 - n + n/[2]) \quad (4)$$

The hypothesis is tested in Figure 5b, where a plot of TSC vs  $n$  shows that (a) the overall value of TSC is 1/4.1 and (b) TSC( $n$ ) is exponential, implying that the isotope effect of 4.1 comes from a number of contributing sites. Figure 5b thus shows that the data for  $k(n)$  can adequately be described by eq 5.

$$(k_n, \text{s}^{-1})^{-1} = (640)^{-1} + \{640/[(1 - n + n/[2])[4.1]^n]\}^{-1} \quad (5)$$

The model corresponding to eq 5 has the following features. (a) In HOH, decarboxylation and product release each have rate constants of  $640 \text{ s}^{-1}$ , as indicated by substrate isotope effects.<sup>4</sup> (b) Decarboxylation generates no solvent isotope effect. (c) Product release generates an overall solvent isotope effect of about 2. (d) The product release isotope effect of 2 results from the cancellation between a normal isotope effect of about 4 (4.1 in eq 5) arising from several loosely bound transition-state sites and an inverse isotope effect of 2 resulting from conversion of a loosely bound reactant-state site ( $\phi$  ca. 0.5) to a "water-like" site in the transition state (as in sulfhydryl addition to pyruvate carbonyl). (e) The overall isotope effect on  $k$  is then, because decarboxylation and product release are equally rate-limiting, the arithmetic mean of the isotope effect on decarboxylation (1.0) and the isotope effect on product release (2.0), i.e., 1.5, as observed. Thus product release, like substrate binding, gives evidence of being coupled to a regulatory sulfhydryl addition to the carbonyl of the regulatory pyruvate.

**Preliminary Model for Regulation and Catalysis.** The indications that sulfhydryl addition to the regulatory pyruvate may function within the catalytic cycle, first during the on-reaction for substrate pyruvate and later during the off-reaction for product acetaldehyde, can be considered in the light of long-standing evidence for the role of hydrophobic features of the active site in catalysis.<sup>13</sup> Such features will obviously be most effective if the active site is sequestered from the external environment during catalysis. *We therefore advance here the hypothesis that sulfhydryl addition-elimination reactions at the regulatory pyruvate may function as engines to drive opening and closing of the active site.* If addition is coupled to opening, then the results for  $k/A$  and  $k/B$  suggest that the enzyme in the SE\* form normally possesses a closed active site. Sulfhydryl addition would then drive the active site open to admit pyruvate. At some point following substrate entry, elimination (apparently rapid and not seen kinetically) would drive closing of the active site to sequester the reactants during decarboxylation. Sulfhydryl addition would again drive the active site open to allow products to escape, with a subsequent elimination closing the site before arrival of substrate for the next cycle.

Although we are currently examining the crystal structures of TDP-dependent enzymes for further evidence on this matter,

it may not be readily resolved by structural examination. The structural alterations involved in opening and closing of the active site could be as large as domain motions of the protein or as small as rotations of a single amino acid side chain. Molecular dynamics approaches may be capable of addressing the question.

### Experimental Section

**Materials.** In Halle, SCPDC was prepared from fresh brewer's yeast obtained from VEB Exportbierbrauerei Wernesgrün (Vogtland). The purified enzyme (33–36 U/mg) was stored frozen in buffered ammonium sulfate solution (0.2 M sodium citrate buffer, pH 5.9, 0.5 M ammonium sulfate at  $-12 \text{ }^\circ\text{C}$ ). In Lawrence, SCPDC was purchased from Sigma (ca. 12 U/mg) and stored at  $4 \text{ }^\circ\text{C}$ . Yeast alcohol dehydrogenase was purchased from Serva (250 U/mg) or Sigma (300–400 U/mg). Sodium pyruvate was purchased from Merck or Sigma. NADH was obtained from VEB Arzneimittelwerk Dresden or Sigma. Deuterium oxide was purchased from VEB Berlin-Chemie (99.86%), BioRad (99.8%), Aldrich (99.8%), or Norell (99.9%). TDP-HCl was from Sigma (96%). All other substances used were of the highest commercially available grade of purification. Buffers were prepared in pure isotopic solvents by dissolution of citric acid and sodium citrate and adjustment of pH(D) with sodium lyoxide solutions (taking pD = meter reading + 0.40).<sup>8,9</sup>

**Steady-State Kinetics.** Decarboxylation rates of pyruvate with SCPDC catalysis were measured spectrophotometrically with coupling of acetaldehyde formation to its reduction to ethanol by alcohol dehydrogenase. The reaction rate was obtained by linear regression of absorbance values at 366 nm (conversion of NADH to NAD<sup>+</sup>) as a function of time in the steady-state (after the activation phase) measured with a Specord M 40 spectrophotometer (VEB Carl Zeiss Jena) or was obtained from absorbance at 340 nm vs time measured with a Cary 118 spectrophotometer interfaced to a Heathkit H-11A computer, 1000 points being collected over 6–7 min. Kinetic parameters were calculated by a distribution-free method, calculations being performed with a HP 9825A desktop computer, or by standard nonlinear least-squares methods.

**Proton Inventory Studies.** In proton inventory studies, the atom fraction of deuterium needed was obtained by mixing appropriate volumes of isotopic waters and sodium citrate buffers in pure isotopic solvents to give the desired final buffer concentration. All reagent solutions were prepared with light water. No differences in reaction rates were observed when the assay was started by addition of substrate or addition of enzyme. A background reaction with a rate of about 2–3 milliabsorbance units/min was generally observed.

**Acknowledgment.** We are happy to thank Shaoxian Sun for much expert help.

**Supplementary Material Available:** Tables of transient and steady-state kinetic parameters as a function of pH(D) in HOH and DOD with figures and experimental description (9 pages). This material is contained in many libraries on microfiche, immediately follows this article in the microfilm version of the journal, and can be ordered from the ACS; see any current masthead page for ordering information.

JA943667S